Synthesis of titanium dioxide precursor by the hydrolysis of titanium oxychloride solution

Le Bideau, P.[a*] ; Richard-Plouet, M.[b] ; Glouannec, P.[a] ; Magueresse, A.[a]; Iya-Sou, D.[b]; Brohan, L.[b]

[a] Univ. Bretagne Sud, IRDL, UMR CNRS 6027, F-56100, Lorient, France
[b] Institut des Matériaux Jean Rouxel (IMN), Université de Nantes, CNRS, F-44322, Nantes, France

*E-mail of the corresponding author: pascal.le-bideau@univ-ubs.fr

Abstract

This communication focuses on the development of an approach to improve the synthesis of [Ti8O12(H2O)24]Cl8.HCl.7H2O crystals which is one of the precursor for titanium dioxide TiO2 particles. This study provides a significant improvement in crystallization kinetics with a production rate increased by a factor nineteen by intensifying heat and mass transfers compared to the process in a close vessel. This enhancement was made possible by the development of a new reactor to control the heat and mass transfers involved. In parallel with the experimental set-up, a numerical model representative of the transfer phenomena was initiated. The first numerical results are encouraging and present a good agreement with the measurements.

Keywords: Heat and mass transfer; Co-desorption, Modelling, Experiment

1. Introduction

Titanium dioxide TiO_2 particles are widely used in various applications. Thanks to its high refractive index, the industrial production of TiO_2 is mainly dedicated to produce pigments as whitening agent in paints [1]. This transition metal oxide is also well known for its n-type semi-conductivity leading to many applications such as gas sensor [2] or solar cell [3]. Additionnally its bandgap close to 3.2 eV gives interesting properties related to its photoactivity such as photocatalysis, self cleaning, light induced superhydrophilicity, among others. Titanium dioxide can be synthesized from various precursors such as alkoxides or inorganic salts. Depending on the pH, single crystals of $[Ti_8O_{12}(H_2O)_{24}]Cl_8.HCl.7H_2O$ were demonstrated to selectively lead to different varieties of nanostructured titanium dioxide [4]. The crystals can be obtained by the hydrolysis of titanium oxychloride solution $TiOCl_2,xHCl,yH_2O$, called aqueous solution of titanium tetrachloride. Due to the reactivity of the latter with water, it may be difficult to properly ensure the reproductibility of syntheses. Therefore a smart strategy is to use $[Ti_8O_{12}(H_2O)_{24}]Cl_8.HCl.7H_2O$ as reactant because of the known composition of the crystals and their solubility in polar solvents. With the adequate air temperature and air humidity conditions, the aqueous solution of titanium tetrachloride reacts to produce those crystals in releasing water and hydrochloric acid in the surrounding environment [5]. The formation process of $[Ti_8O_{12}(H_2O)_{24}]Cl_8.HCl.7H_2O$ is a complex process involving several species and several reaction kinetics. The aim here is to treat mass and heat problems in a highly reactive and deformable medium in order to get insight in the crystallization mechanisms and further optimize the process in order to accelerate the crystallisation. Figure 1 presents a simplified view of the different phenomena involved during the formation of $[Ti_8O_{12}(H_2O)_{24}]Cl_8.HCl.7H_2O$. The commercial solution is initially composed of 3 species: $TiOCl_2$, H_2O and HCl which react under particular ambient conditions of temperature and humidity to form $[Ti_8O_{12}(H_2O)_{24}]Cl_8.HCl.7H_2O$. During the process, $TiOCl_2$ and H_2O species are consumed while HCl and $[Ti_8O_{12}(H_2O)_{24}]Cl_8.HCl.7H_2O$ species are produced. At the solution/air interface, H_2O and HCl, are transferred to the ambient environment by evaporation. This evaporation causes on the one hand a variation in the volume of the mixture (shrinkage) and on the other hand a modification in the thermal and mass balance leading to temperature and concentration gradients within the mixture.
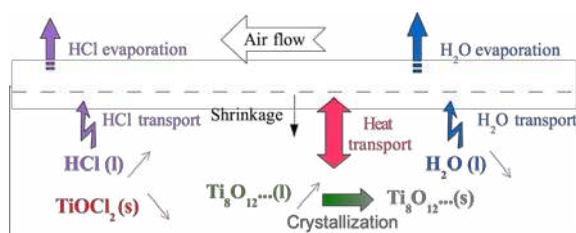

Fig. 1 Schematic description of physical phenomena

After a brief presentation of the titanium oxychloride solution, the static reactor, the laminar air flow reactor and the metrology used are described. A numerical model predicting the mass behavior of the solution during the first stage of process (before the crystallization kinetic) is presented. The experimental results obtained with the static and dynamic configurations are then discussed and show the capabilities to intensify the crystal production. The first numerical results are finally introduced.

2. Materials and Methods

2.1. Product description

At ambient temperature (T = 25°C), titanium oxychloride solution (Cristal) is a viscous, yellow liquid which is highly hygroscopic and very acidic (pH far below 1).The titanium oxychloride solution encloses [$TiOCl_2(H_2O)_2$] species dissolved in aqueous hydrochloric solution with the following composition: $1.375HCl, 5H_2O$. This solution is composed (in percentage by weight) of 54.9 % of the initial species ($TiOCl_2(H_2O)_2$), 16.1 % of HCl and 29 % of water. Based on this composition, the solvent proportion is 64,2 % of water and 35.8 % of HCl. This formulation was validated by placing the commercial solution in an atmosphere containing 36 %wt HCl and verifying the mass balance. In classical conditions (T = 25 °C and HR ≈ 50 %), HCl-H_2O co-desorption leads to the crystallisation of [$Ti_8O_{12}(H_2O)_{24}$]$Cl_8.HCl.7H_2O$. This crystals formation requires a mass loss of 41.6 %wt : 15.2 %wt water and 26.4 %wt HCl.

2.2. Crystallization reactors

2.2.1. Static reactor

The first syntheses were performed in a dessiccator containing a crystallizer filled with 2 mL of titanium oxychloride solution (solution height approx. 2 mm). A H_2SO_4/H_2O mixture is deposited at the dessiccator base in order to set the relative humidity close to 55 % at ambient temperature. Mass variations and crystals formation are monitored by carrying out discontinuous successive *ex situ* measurements.

2.2.2. Laminar air flow reactor

In order to intensify the massive exchanges and thus the production rate of crystals, a new experimental set-up was developed (Fig. 2). It consists in a rectangular PMMA duct (height: 11 cm, width: 17 cm) in which a PMMA crucible (10 cm x 10 cm) is placed. Air flow is blown parallel to the surface of the crucible containing the solution. This crucible which contained 22 mL of titanium oxychloride solution (solution height approx. 2.5 mm) is positioned on a weighing system that allows continuous mass monitoring. A heating system stuck below the crucible allowed us to control the solution temperature. The inlet air

conditions (temperature and relative humidity) are controlled by an upstream system equipped with a heat pump and a humidifier. Temperature sensors placed at upstream, downstream track air temperature variations. Other thermocouples are also stuck on heating element and positioned in the solution. A velocity sensor measures the air speed at the inlet of the duct. All these sensors are connected to a data acquisition system. In the same time, images of the solutions are recorded to track the shrinkage and the crystals formation.
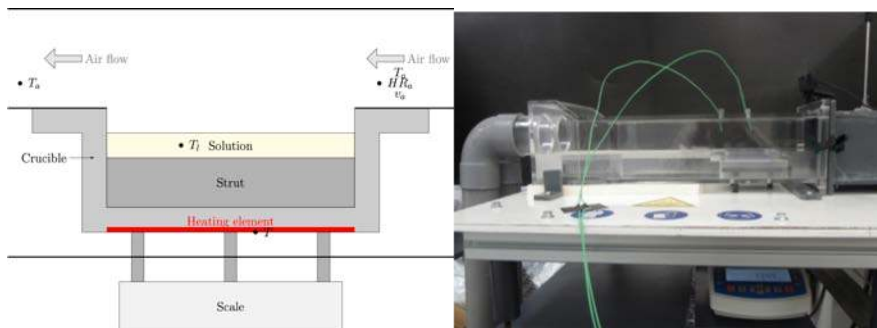

Fig. 2 Laminar air flow reactors description

2.3. Numerical modeling

First, a numerical approach is initiated to predict the mass loss of the solution during the first step of the process (before the beginning of the crystallization). This model based on the mass conservation equations written for the solvents (HCl and H_2O) and the solute [$TiOCl_2(H_2O)_2$] should predict solvent concentrations as a function of the surrounding air conditions and/or the temperature of solution imposed by the heating system. The solution temperature is not computed but imposed based on experimental measurements.

The model assumptions are as follows: the initial solution (homogeneous) consists of 3 species [$TiOCl_2(H_2O)$]$_2$, H_2O and HCl; the species transport only takes place by diffusion (Fick's diffusion); the species transfer is assumed to be one-dimensional; the shrinkage is assumed to be linear; water reacts with the solute and is consumed to form HCl species.

2.3.1. Governing equations

The application of mass convervation principle leads to write the following equations:

$$\frac{\partial \rho_s}{\partial t} + \mathrm{div}(\rho_s \overrightarrow{v_s}) = 0 \tag{1}$$

$$\frac{\partial \rho_i}{\partial t} + \mathrm{div}(\rho_i \overrightarrow{v_s}) = -\mathrm{div}(\overrightarrow{J_i}) + S_i \tag{2}$$

With ρ the mass density (kg m^{-3}), J the mass flow (kg m^{-2} s^{-1}), S the mass source (kg m^{-3} s^{-1}) and v the shrinkage velocity (m s^{-1}). The subscript i refers to HCl noted A or water noted W.

2.3.2.   *Boundaries conditions*

At the interface between the solution and the crucible base, no mass transfers occur:

$$-\mathbf{n}(\vec{J_l}) = 0 \tag{4}$$

At the interface between the solution and the air flow, mass transfers depend on the difference of vapor densities between the product at the surface (surf) and the surrounding air (a):

$$-\mathbf{n}(\vec{J_l}) = h_m\left(\rho^v_{i,surf} - \rho^v_{i,a}\right) \tag{5}$$

With h_m the mass transfer coefficient (m s^{-1}).

Water vapor and hydrochloric acid vapor are assumed to be ideal gas and the previous relation is expressed as a function of the partial pressure at the product surface and the partial vapor pressure of the ambient atmosphere. Considering that the initial complex does not affect the HCl/water mixture, it can be assumed that the partial vapor pressures of HCl/water mixture only depend on the temperature and concentration of HCl [6].

3.   **Results and discussion**

3.1.   **Static syntheses**

Various syntheses performed at room temperature and with a relative humidity set at 55 % present similar and repeatable behaviors. In figure 3, a first mass loss is observed during the first hours of drying caused by a significant release of solvents (HCl and water). This first stage goes on until the mass loss reaches about 15 % (≈ 15 h). At this stage, the first crystalline seeds appear and the crystallization kinetic accelerates. Co-desorption is then slowed down as long as the crystals grow and agglomerate. At the end of the process, the mass loss corresponds to about 41 %wt of the initial mass which matches with the predicted value by chemical equations. Under these conditions, about 25 days are required to form the crystals with a production rate per unit surface of about 630 g/(week.m^2).
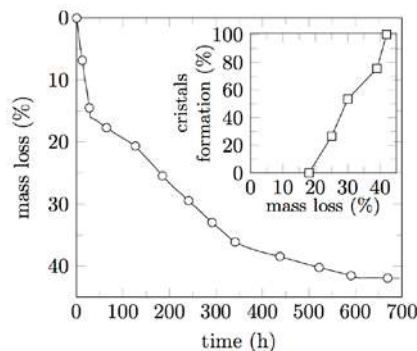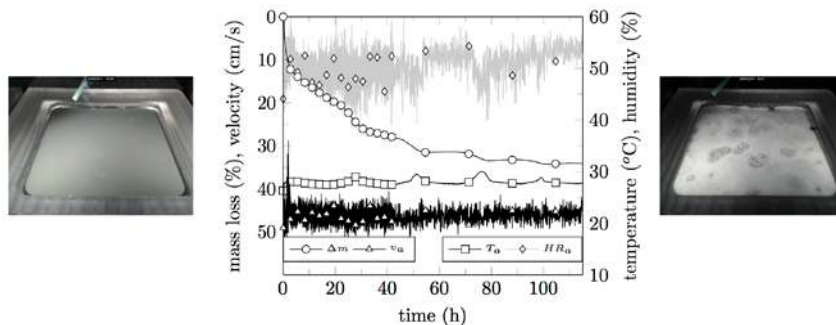

Fig. 3 Mass loss and crystals formation during static syntheses
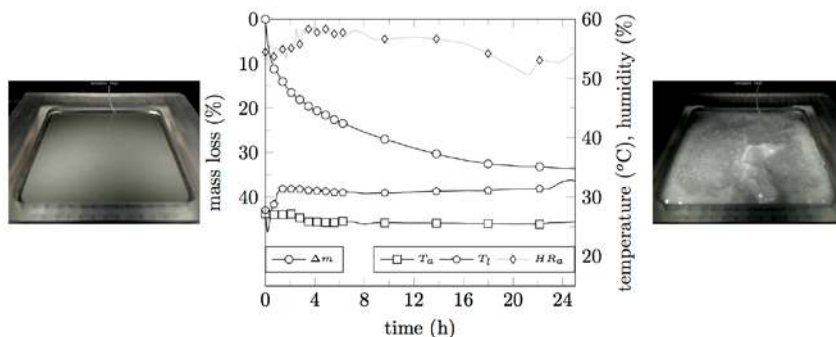
3.2. Dynamic syntheses

In a second step, syntheses were performed using the laminar airflow reactor. First experiments are carried out without direct heating (Fig. 4). The air temperature (T_a) is set to 28 °C and relative humidity (HR_a) varies between 45 % and 55 %. The air velocity (v_a) is set to about 0.45 m s^{-1}.

Fig. 4 Dynamic synthesis without direct heating, images of the crucible before (left) and after (right) crystallization, evolution of the mass loss, temperature and relative humidity with time (middle)

In these conditions, the first stage which corresponds to a mass loss (Δm) of 15 % is completed in about 8 h. The stationary phase is reached after 110 h (> 4 days). At the end of process, the mass loss corresponds to about 35 %wt and not 41 % as expected. This result can be explained by a crystallization at the surface which prevents the mass diffusion (HCl and water) from the medium toward the surface. The production rate of crystals is about 2.2 kg/(week.m^2) being more than 3 times the static production rate.

In order to intensify the mass transfer and thus reduce the synthesis time experiments are carried out with a direct heating (Fig. 5). The air temperature (T_a) is set to 27 °C and relative humidity (HR_a) varies between 50 % and 60 %. The air velocity (v_a) is set to 0.45 m s^{-1}.

**Fig. 5 Dynamic synthesis with direct heating, images of the crucible before (left) and after (right) crystallization, evolution of the mass loss, temperature and relative humidity with time (middle)**

The solution temperature (T_l) varies from 27°C to 32°C during the first two hours due to switching on of the heating element (heating element temperature about 42°C). The first stage which corresponds to a mass loss of 15 % is completed within about 2 h. The stationary phase is reached after 24 h. At the end of process, the mass loss corresponds to about 34 %wt which is very similar to the value obtained in the previous case (without heating element). In this condition, the production rate of crystals is about 12 kg/(week.m^2), i.e., 19 times the production rate achieved in static mode.

3.3.   Numerical results

The numerical model is tested for the dynamic configuration in the first hours of the synthesis process (before the beginning of the crystallization). The predicted mass losses are compared with the experimental ones for the tests performed without and with direct heating (Fig. 6). For these two configurations, the numerical results present a good agreement with the measurements. Experimentally, the solution density varies from 1.58 at the initial state to 1.5 when the mass loss reaches 20 %.
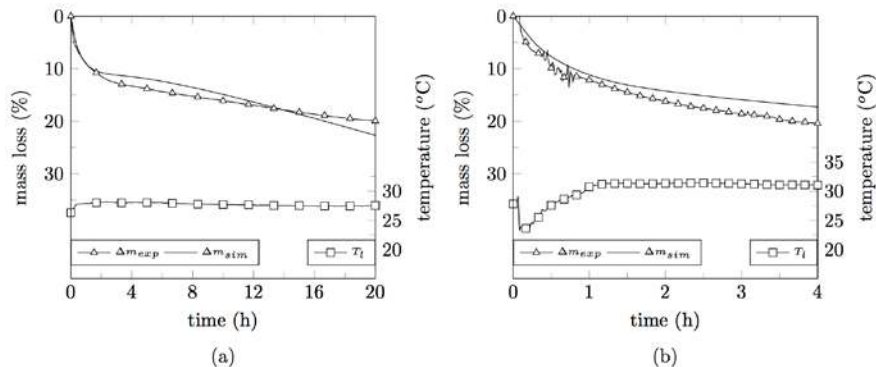
Fig. 6 Evolution of the temperature (open square), experimental (open triangle) and simulated (line) mass losses without (a) and with (b) direct heating, as a function of time

4.   Conclusions

Under static conditions, the production of $[Ti_8O_{12}(H_2O)_{24}]Cl_8.HCl.7H_2O$ crystals requires several weeks. In order to improve the production rate, a laminar air flow reactor with temperature and humidity controls was developed. With adequate conditions (air and solution temperature and air relative humidity), a significant improvement in the crystals production was obtained from 630 g/(week.m^2) to 12 kg/(week.m^2). These encouraging results could be improved in future by studying more extensively the temperature/humidity pair providing the best yield. In parallel, a numerical model describing mass transfers (before crystallization began) was initiated. The first numerical results correctly reflect experimental observations and encourage further development.

5.   Acknowledgement

6.   References

[1]   Pfaff, G.;Reynders, P. Angle-dependent optical effects deriving from submicron structures of films and pigments. Chemical Reviews 1999, 99(7), 1963-1982.

[2]   Zhu, Y.; Shi, J.; Zhang, Z.; Zhang, C., Zhang, X. Development of a gas sensor utilizing chemiluminescence onf nanosized titatnium dioxide. Analytical Chemistry 2002, 74(1), 120-124.

[3]   Carp, O.; Huisman, C.L.; Reller, A. Photoinduced reactivity of titanium dioxide. Progess in Solid State Chemistry 2004, 32 (1-2), 33-177.

[4]   Liu, C.E.; Rouet, A.; Sutrisno, H.; Puzenat, E.; Terrisse, H.; Brohan, L.; Richard-Plouet, M. Low temperature synthesis of nanocrystallizes titanium oxides with layered of tridimensional frameworks, from $[Ti_8O_{12}(H_2O)_{24}]Cl_8.HCl.7H_2O$. Chemistry of Material 2008, 20, 4739-4748.

[5]   Brohan, L.; Sutrisno, H.; Puzenat, E.; Rouet, A.; Terrisse, H. French CNRS Patent 0305619, May 9, 2003; International Publication WO 2004/101436 A2, Nov 25, 2004; European CNRS patent (EP) 04 742 604.4, Nov 24, 2005; Japan (JP) CNRS Patent 2006-530327, Oct 16, 2006; United States (US) CNRS Patent 018344/0578, Feb 4, 2006.

[6]   Perry, R.H.; Green, D.W. Perry's chemical engineers'handbook, McGraw-Hill: New York, 1999.